

Oxygen Nonstoichiometry in Li_2MnO_3 : An Alternative Explanation for Its Anomalous Electrochemical Activity

D. Pasero, V. McLaren, S. de Souza, and A. R. West*

Department of Engineering Materials, The University of Sheffield, Mappin Street, Sheffield, S1 3JD, U.K.

Received July 30, 2004. Revised Manuscript Received October 4, 2004

Li_2MnO_3 loses oxygen, reversibly, on heating above $\sim 600^\circ\text{C}$. By 1100°C , 1% of the oxygen has been lost, giving a stoichiometry of $\text{Li}_2\text{MnO}_{2.97}$. Depending on the synthesis conditions, materials with a range of oxygen contents may be produced. Associated with the variable oxygen content, partial reduction of Mn^{4+} to Mn^{3+} occurs, as demonstrated by a direct correlation between electrochemical capacity, when used as a cathode in a rechargeable Li test cell, and oxygen content.

Introduction

As part of a wider search for cathode materials for lithium ion rechargeable batteries, lithium manganates such as LiMn_2O_4 ^{1–3} have very attractive electrochemical properties as well as being cheaper and less toxic than the commercially used intercalation compound LiCoO_2 .⁴ A related compound, Li_2MnO_3 , has recently been the subject of several investigations due to its unexpected electrochemical activity.^{5,6} Because manganese in Li_2MnO_3 is present only in the tetravalent state, it is not expected that any Li^+ ions can be extracted electrochemically from the structure because it is generally accepted that manganese cannot be oxidized to Mn^{5+} in an octahedral environment.⁷ However, several studies have reported that Li^+ extraction takes place with moderately high specific capacities (above 150 mAh g^{-1}) in the 2.5–4.5 V potential window, in samples prepared by both solid-state reaction⁵ and acid-leaching.⁸ The cyclability of these materials was reported to be poor, although acid-leached samples exhibited improved performance. The cause of this anomalous activity is still unclear, and several mechanisms have been put forward. Some authors have suggested that oxidation to Mn^{5+} may indeed take place,⁶ whereas in a study on Ni-doped Li_2MnO_3 , this behavior was attributed to the simultaneous extraction of O^{2-} during cycling.⁹ Other authors found that exchange of Li^+ by H^+ occurred at the positive electrode, linked to oxidation of the electrolyte at the cathode, giving rise to the observed capacity.¹⁰

Li_2MnO_3 possesses an ordered layered rock-salt structure, space group $C2/c$ [JCPDS card 27-1252]. It consists of alternating layers of octahedral Li and mixed Li, Mn layers as illustrated in the conventional notation for ABO_2 layered materials by the formula $\text{Li}[\text{Li}_{1/3}\text{Mn}_{2/3}]\text{O}_2$. In none of the previously published reports on Li_2MnO_3 has its oxygen content been measured, and it has always been assumed to be oxygen-stoichiometric. From this assumption, the oxidation state of Mn in Li_2MnO_3 is Mn^{4+} . By contrast, it is well-established that the oxygen content of the spinel, LiMn_2O_4 , is variable, especially at high temperatures, $> 800^\circ\text{C}$, where oxygen deficiency occurs, and at low temperatures, where oxygen-rich spinels on the join LiMn_2O_4 – $\text{Li}_2\text{Mn}_4\text{O}_9$ have been prepared.¹¹ Oxygen nonstoichiometry occurs widely in other materials, such as the perovskite-related superconductor $\text{YBa}_2\text{Cu}_3\text{O}_\delta$ ¹² and perovskites such as NdMnO_δ .¹³ Here, we report the first occurrence of oxygen nonstoichiometry in a rock-salt-related complex oxide, Li_2MnO_3 , and show that this is a prime cause for electrochemical activity in Li_2MnO_3 .

Experimental Section

Stoichiometric mixtures of dried starting materials Li_2CO_3 and MnO_2 (Sigma Aldrich), all reagent grade, were ground intimately in an agate pestle and mortar and fired in air, initially at 650°C for 2 h to expel CO_2 , followed by 900°C for 3 days with intermittent regrinding (hereafter named as-prepared, P). Portions were then reheated and quenched from higher temperatures (1000 and 1100°C) into Hg (hereafter named Q1000 and Q1100). A portion of as-prepared sample was also reheated in a Morris High Oxygen Pressure furnace at 120 atm O_2 at 700°C for 3 h, followed by slow cool under pressure (hereafter named HOP).

Powder X-ray diffraction, XRD, used a Philips 1710 diffractometer, $\text{Cu K}\alpha$ radiation, scan range $15^\circ < 2\theta < 80^\circ$ in steps of 0.02° , and Si as internal standard. Indexing and structure refinement used the WinXPow software package. Thermogravimetric analysis, TG, used a Perkin-Elmer Pyris 1 TGA with autosampler. Samples

* Corresponding author. E-mail: a.r.west@sheffield.ac.uk.

- (1) Ohzuku, T.; Kitagawa, M.; Hirai, T. *J. Electrochem. Soc.* **1990**, *137*, 769.
- (2) Tarascon, J.-M.; Wang, E.; Shokoohi, F. K.; McKinnon, W. R.; Colson, S. *J. Electrochem. Soc.* **1991**, *138*, 2859.
- (3) Yamada, A.; Miura, K.; Hinokuma, K.; Tanaka, M. *J. Electrochem. Soc.* **1995**, *142*, 2149.
- (4) Mizushima, K.; Jones, P. C.; Wiseman, P. C.; Goodenough, J. B. *Mater. Res. Bull.* **1980**, *15*, 783.
- (5) Robertson, A. D.; Bruce, P. G. *Chem. Commun.* **2002**, 23, 2790.
- (6) Kalyani, P.; Chitra, S.; Mohan, T.; Gopukumar, S. *J. Power Sources* **1999**, *80*, 103.
- (7) Amundsen, B.; Paulsen, J. *Adv. Mater.* **2001**, *13*, 943.
- (8) Paik, Y.; Grey, C. P.; Johnson, C. S.; Kim, J.-S.; Thackeray, M. M. *Chem. Mater.* **2002**, *14*, 5109.
- (9) Lu, Z.; Dahn, J. R. *J. Electrochem. Soc.* **2002**, *149*, A815.

- (10) Robertson, A. D.; Armstrong, A. R.; Paterson, A. J.; Duncan, M. J.; Bruce, P. G. *J. Mater. Chem.* **2003**, *13*, 2367.
- (11) Masquelier, C.; Tabuchi, M.; Ado, K.; Kanno, R.; Kobayashi, Y.; Maki, Y.; Nakamura, O.; Goodenough, J. B. *J. Solid State Chem.* **1996**, *123*, 255.
- (12) Goodenough, J. B. *Mater. Res. Bull.* **1988**, *23*, 401.
- (13) Maguire, E. T.; Coats, A. M.; Skakle, J. M. S.; West, A. R. *J. Mater. Chem.* **1999**, *9*, 1337.

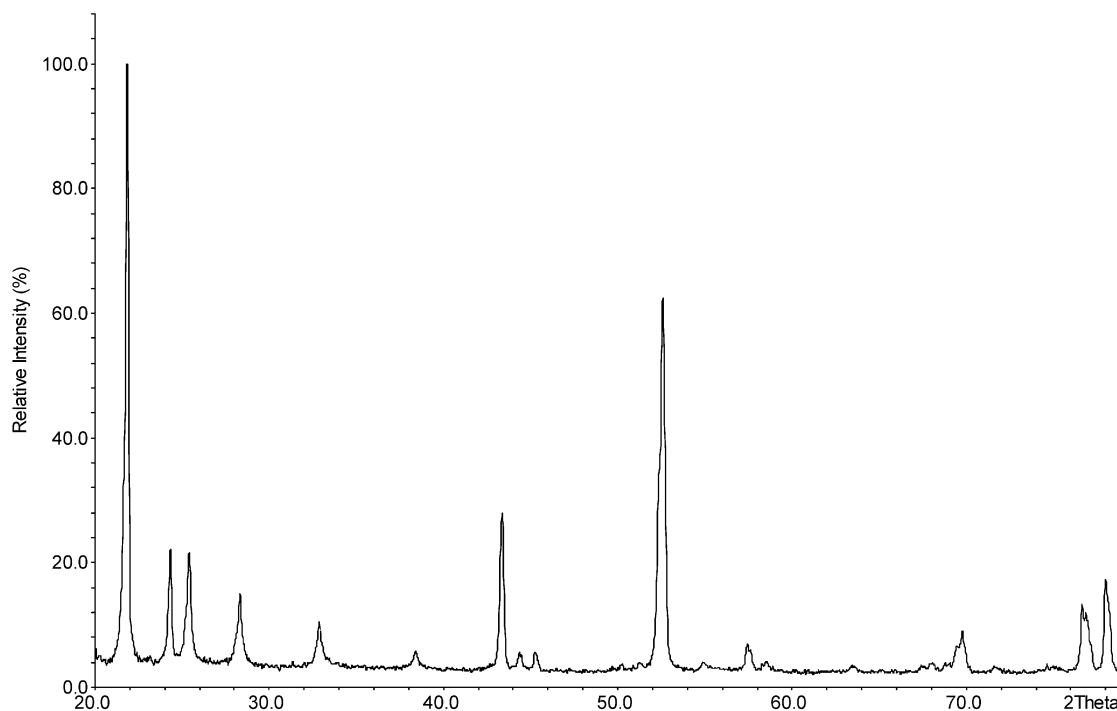


Figure 1. XRD profile of as-prepared sample P.

were heated at 10 °C/min to 1000 °C and then cooled at the same rate to room temperature. The average oxidation state of manganese was measured by a titration method using $\text{K}_2\text{Cr}_2\text{O}_7/\text{Fe}^{2+}$.¹⁴ Samples were dissolved in acid (6 M $\text{H}_3\text{PO}_4/\text{H}_2\text{SO}_4$) in the presence of excess Fe^{2+} . Back-titration was performed under N_2 on the unreacted Fe^{2+} with $\text{K}_2\text{Cr}_2\text{O}_7$.

To make positive electrodes for electrochemical testing, an 80:10:10 wt % mix of active cathode material, carbon black, and PVdF was suspended in THF (Sigma Aldrich), and a thin film was deposited on top of an aluminum foil, 0.05 mm thick (Sigma Aldrich). Coin cells (2325) were constructed under Ar in a glovebox, using parts and a press provided by the National Research Council of Canada. Li-metal was used as negative electrode, and 1 M LiPF_6 in EC:DMC = 1:1 (Merck) was used as the electrolyte. Electrochemical testing used an 8-channel VMP system (Bio-Logic) with galvanostatic measurements at room temperature, at the low-rate C/30 in the potential window 2.5–4.7 V. Because any oxygen deficiency, δ , leads to the creation of $2\delta \text{ Mn}^{3+}$ cations per unit formula in $\text{Li}_2\text{Mn}^{4+}_{1-2\delta}\text{Mn}^{3+}_{2\delta}\text{O}_{3-\delta}$, the resulting specific capacity associated with oxidation of Mn^{3+} to Mn^{4+} is given by Faraday's Law:

$$Q = 2\delta F / M_{\text{Li}_2\text{MnO}_{3-\delta}} \text{ in C g}^{-1} = 2\delta F / 3.6 M_{\text{Li}_2\text{MnO}_{3-\delta}} \text{ in mAh g}^{-1} \quad (1)$$

where $F = 9.649 \times 10^4 \text{ C mol}^{-1}$. This equation therefore relates the oxygen deficiency, δ , to the measured capacity, Q .

The ac impedance measurements were performed using a Solartron 1260 Impedance analyzer over the frequency range 0.01 Hz to 1 MHz. Samples were in the form of ceramic disks sintered at various temperatures; Au electrodes were mounted onto the sample using an InGa paste at room temperature.

Results and Discussion

X-ray Powder Diffraction, XRD. The XRD data for the as-prepared sample, P, Figure 1, were fully indexed on a

monoclinic unit cell: $a = 4.9257(4) \text{ \AA}$, $b = 8.5250(14) \text{ \AA}$, $c = 9.6278(14) \text{ \AA}$, $\beta = 99.576^\circ(12)$. This compares reasonably well with the reported unit cell parameters: $a = 4.928 \text{ \AA}$, $b = 8.533 \text{ \AA}$, $c = 9.604 \text{ \AA}$, $\beta = 99.5^\circ$.¹⁵ Samples quenched from 1000 and 1100 °C and annealed in high-pressure oxygen showed essentially the same XRD patterns, but accurate lattice parameter measurements showed small shifts with increasing quench temperature. Lattice parameters and cell volume increased with increasing temperature, consistent with loss of oxygen (see later), reduction in average valence of Mn, and hence lengthening of Mn–O bonds.

The similarity in the XRD patterns of the various samples illustrates the stability of the structure of Li_2MnO_3 to at least 1100 °C. The structurally related Li_2TiO_3 shows an order–disorder transition at 1213 °C.¹⁶ To determine whether a similar transition may occur in Li_2MnO_3 , solid solutions of general formula $\text{Li}_2(\text{Ti}_{1-x}\text{Mn}_x)\text{O}_3$ were prepared; by DTA, the phase transformation temperature increased gradually with x to 1220 °C at $x = 0.1$; experiments were not carried out at high x values, due to the high temperatures involved and the possibility of damage to/contamination of the DTA instrument; these results do, however, indicate the possibility of an order–disorder transition in Li_2MnO_3 but at a temperature significantly greater than 1200 °C.

Thermogravimetry, TG. Initial TG measurements showed a reversible loss/gain in weight on heating the samples above ~800 °C. From their reversibility, and in particular the different behavior in different atmospheres, it was clear that the samples had variable oxygen content. To achieve a reference composition, samples were heated and slowly cooled in high-pressure oxygen with the assumption that the products would correspond to stoichiometric Li_2MnO_3 .

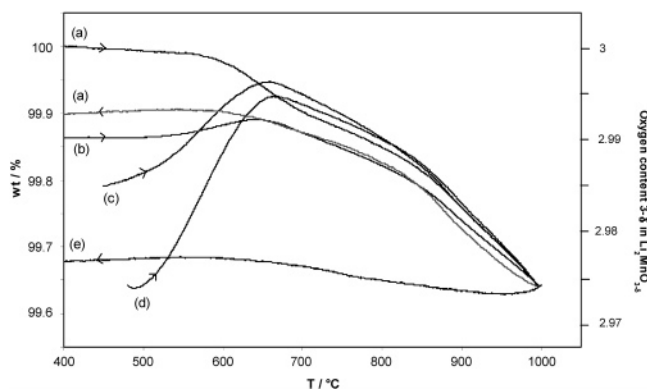
(15) Jansen, M.; Hoppe, R. *Z. Anorg. Allg. Chem.* **1973**, 397, 279.

(16) Izquierdo, G.; West, A. R. *Mater. Res. Bull.* **1980**, 15, 1655.

(14) Scaccia, S.; Carewska, M. *Anal. Chim. Acta* **2002**, 455, 35.

Table 1. Average Oxidation State of Mn and Oxygen Content $3 - \delta$ in $\text{Li}_2\text{MnO}_{3-\delta}$ Obtained by Electrochemistry, TG, and Titration Measurements

sample	electrochemistry data			TG data		titration data	
	capacity measured after 20 discharges/mAh/ g ± 0.5	average oxidation state of Mn ± 0.005	oxygen content $3 - \delta$ ± 0.003	average oxidation state of Mn ± 0.005	oxygen content $3 - \delta$ ± 0.003	average oxidation state of Mn ± 0.02	oxygen content $3 - \delta$ ± 0.01
HOP	0.5	3.998	2.999	4.000	3.000	4.02	3.01
P	4	3.982	2.991	3.982	2.991	4.00	3.00
Q1000	6	3.973	2.987	3.968	2.984		
Q1100	13	3.943	2.971	3.946	2.973	3.97	2.98

**Figure 2.** TG data in air for $\text{Li}_2\text{MnO}_{3-\delta}$ samples (a) in HOP at 120 atm O_2 , 700 °C for 3 h, (b) as-prepared, (c) quenched from 1000 °C, and (d) quenched from 1100 °C. Data in (e) are for a sample cooled from 1000 °C in N_2 . It is assumed that sample (a) had stoichiometry $\delta = 0$ at 25 °C and that all samples have the same δ value when heated in air at 1000 °C.

Conditions used were 700 °C, 120 atm O_2 , 3 h, followed by a programmed cool at 1 °C min^{-1} . Due to the nature of the Morris furnace used, the sample pressure gradually reduced during cooling to approx ~ 28 atm at room temperature.

It is assumed that this high-pressure treated sample has the final stoichiometry Li_2MnO_3 , and, therefore, all TG results are scaled according to this. In addition, because equilibration of oxygen content appears to occur rapidly above ~ 800 °C, it was assumed, as a second point of reference, that all samples heated in air had the same oxygen content at 1000 °C.

With these assumptions, TG data for a selection of samples are shown in Figure 2. In (a) are the data for the high-pressure treated sample; oxygen loss commences at about 550 °C and continues gradually until the highest temperature reached, 1000 °C. On cooling, weight gain is essentially fully reversible until ~ 700 °C. The original weight is not fully recovered due to the relatively slow rate of oxygen uptake below ~ 700 °C. Data are shown in (b) for the sample prepared at 900 °C. In this case, the sample shows a modest increase in weight in the range 550–650 °C before losing weight at higher temperature. Data on cooling (not shown) are essentially reversible, and the final weight corresponds to that on heating the sample at ~ 650 °C. In (c,d), data are shown for the sample quenched from 1000 and 1100 °C in air, respectively. In these cases, a major increase in weight occurs between approximately 500 and 650 °C, after which the usual pattern of weight loss behavior is observed. Data for the same as-prepared sample, but cooled in nitrogen, are shown in (e); little of the weight lost is subsequently recovered on cooling.

From these results, we may draw the following conclusions. First, Li_2MnO_3 loses oxygen reversibly at high temperatures and oxygen loss continues to at least 1100 °C. Second, the extent of the reversibility of oxygen loss/uptake depends on the cooling rate. Thus, in the as-received sample cooled in air and, in particular, the samples quenched from 1000 and 1100 °C, the samples have not fully oxygenated during cooling; instead, the samples are sufficiently oxygen-deficient that during the heating cycle of TG, a significant increase in weight occurs due to oxygen absorption at ~ 600 °C. Third, there is no evidence of volatilization of Li_2O at high temperatures; if this occurred, it would be evident by irreversibility of weight loss/weight gain on cycling. As the data for the samples heated in air and N_2 demonstrate, the entire TG cycle can be explained on the basis of variation in oxygen content alone. We conclude, therefore, that samples can be satisfactorily heated to 1100 °C, at least, without Li_2O loss occurring; above ~ 600 °C, Li_2MnO_3 is increasingly oxygen-deficient, and equilibration is rapid for temperatures above ~ 700 °C. The most oxygen-deficient sample prepared so far is that quenched from 1100 °C, with an approximate composition $\text{Li}_2\text{MnO}_{2.97}$, which retains the basic crystal structure of the parent Li_2MnO_3 .

Titration Results. Results of titration analyses, presented as both average oxidation state of Mn and oxygen content, $3 - \delta$, are given in Table 1, together with summarized results of TG analyses and electrochemical data (see next section) for comparison. Within errors, which are considerably larger for the titration analyses, similar conclusions are obtained; the HOP sample is essentially oxygen-stoichiometric, and about 1% of the oxygen is lost from Li_2MnO_3 on heating to 1100 °C.

Electrochemical Results. Charge–discharge experiments on cells containing $\text{Li}_2\text{MnO}_{3-\delta}$, $2.97 \leq 3 - \delta \leq 3.00$, as the active component of the cathode were carried out for up to 50 cycles. Results for four samples, showing the capacity on discharge, are given in Figure 3. There is a very clear correlation between the degree of oxygen nonstoichiometry and the discharge capacity. For the HOP sample of essential composition Li_2MnO_3 , the discharge capacity levels off at < 1 mAh g^{-1} , whereas, for sample Q1100, the largest capacity is obtained with a value ~ 13 mAh g^{-1} . Capacity values were converted to oxygen contents and average Mn oxidation state and are listed in Table 1. Within errors, the values obtained are the same as those obtained by TG.

A selection of dQ/dV versus V profiles over the range 2.5–4.7 V is shown for sample P in Figure 4. Initially, peaks are seen at ~ 4.4 V on charging and ~ 4.25 V on discharging,

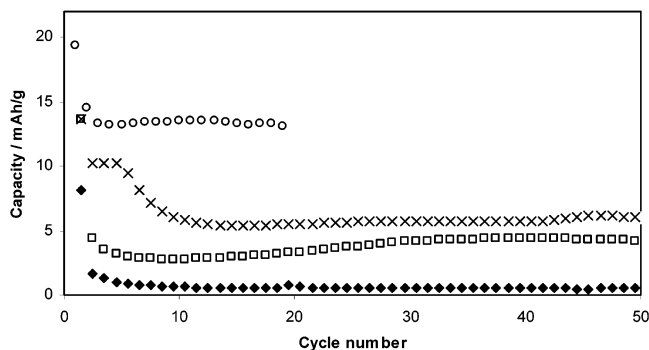


Figure 3. Capacity retention profile of $\text{Li}_2\text{MnO}_{3-\delta}$ samples quenched from 1100 °C (○), quenched from 1000 °C (×), as-prepared (□), and heated in 120 atm O_2 at 700 °C for 3 h (◆).

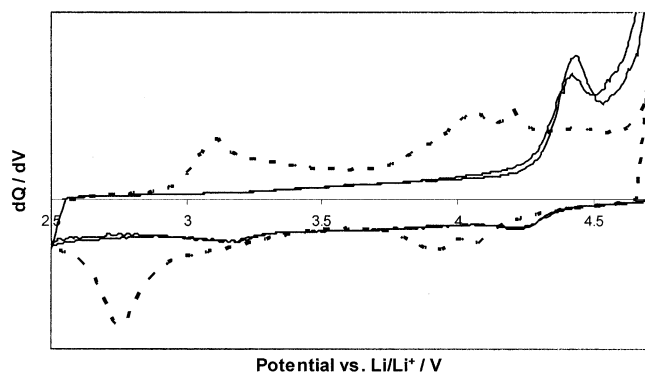


Figure 4. dQ/dV plot for as-prepared sample P; solid line, cycles 2 and 3; dashed line, cycle 75.

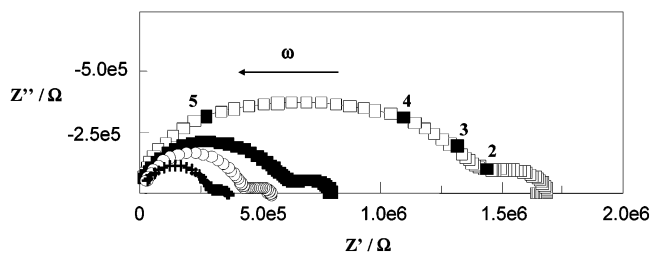


Figure 5. ac impedance data for sample Q1000 collected at 125 °C (□), 150 °C (■), 180 °C (○), and 200 °C (+); selected frequencies, as $\log f/\text{Hz}$, are marked.

but after repeated cycling, the profile changes to give two peaks on charging at ~ 3.2 and $4.0\text{--}4.2$ V and two on discharging at 2.7 and $3.9\text{--}4.1$ V.

This latter set of peaks is very similar to that observed during cycling of LiMn_2O_4 and is attributable to the $\text{Mn}^{3+/4+}$ redox couple in the spinel environment. It is possible, therefore, that a topotactic transformation from the rock-salt structure of Li_2MnO_3 to the spinel structure of LiMn_2O_4 occurs during cycling and, especially, is associated with a reduction in the cation:oxygen ratio on deintercalation of Li. A similar transformation occurs on cycling LiMnO_2 .¹⁷

The electrical conductivity of pelleted samples with different oxygen contents was determined by impedance analysis; impedance complex plane plots, Figure 5, showed a main arc attributed to the bulk of the sample (with an

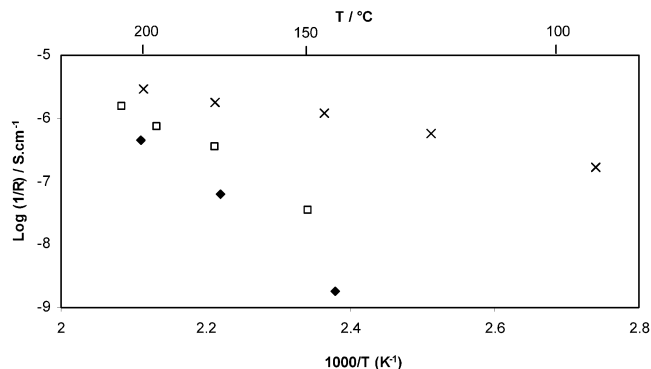


Figure 6. Conductivity versus reciprocal temperature of samples quenched from 1000 °C (×), as-prepared (□), and heated in 120 atm O_2 at 700 °C for 3 h (◆). Activation energies are 0.11, 1.28, and 1.36 eV, respectively.

associated capacitance of 1.2×10^{-11} F) together with a small low-frequency arc attributed to either a grain boundary response or an electrode-sample contact impedance (capacitance 1.1×10^{-9} F). Similar response was seen for all samples.

Bulk conductivity values were extracted from the intercept of the main arc on the Z' axis and are shown plotted in Arrhenius format in Figure 6. With increasing oxygen nonstoichiometry, the conductivity at any temperature increases and the activation energy for conduction decreases. This can be explained by the increase in mixed valence states of Mn with sample reduction and, hence, the increased ease of electron hopping between adjacent Mn ions.

Conclusions

The results presented here demonstrate conclusively that Li_2MnO_3 has variable oxygen content; the actual value in a given sample is likely to depend on synthesis conditions. Structural studies are required to determine whether a random distribution of vacancies in the oxygen sublattice occurs or whether there are any structural complexities such as defect clustering or superstructure formation.

The degree of oxygen nonstoichiometry was determined by three independent methods, with generally excellent agreement between the results. A direct consequence of oxygen nonstoichiometry is a partial reduction of Mn^{4+} to Mn^{3+} to preserve charge balance. This leads to a dramatic increase in electronic conductivity associated with the possibility of electron hopping between the mixed valence states of Mn.

It also leads to the occurrence of significant electrochemical activity in reversible deintercalation/intercalation of Li. Various hypotheses have been put forward in the literature to account for electrochemical activity in Li_2MnO_3 . Results presented here indicate that oxygen nonstoichiometry, leading to the presence of Mn^{3+} , is a previously unrecognized, but major, cause of electrochemical activity.

Acknowledgment. We thank the EPSRC for financial support.

(17) Bruce, P. G.; Armstrong, A. R.; Gitzendanner, R. I. *J. Mater. Chem.* **1999**, *9*, 193.